analytical chemistry

Article

pubs.acs.org/ac

Sensitive Chemiluminescent Imaging for Chemoselective Analysis of Glycan Expression on Living Cells Using a Multifunctional Nanoprobe

En Han, Lin Ding, Ruocan Qian, Lei Bao, and Huangxian Ju*

State Key Laboratory of Analytical Chemistry for Life Science, Department of Chemistry, Nanjing University, Nanjing 210093, China

ABSTRACT: A novel sensitive chemiluminescent (CL) imaging method was developed for in situ monitoring of cell surface glycan expression through chemoselective labeling of carbohydrate motifs and then binding to a multifunctional nanoprobe. The nanoprobe was fabricated by assembling biotin-DNA and a large amount of horseradish peroxidase (HRP) on gold nanoparticles (AuNPs). The chemoselective labeling was performed by selective oxidization of the hydroxyl sites of sialyl and galactosyl groups on cell surfaces into aldehydes by periodate and galactose oxidase, respectively, and then aniline-catalyzed hydrazone ligation with biotin hydrazide for specific recognition to avidin. With the biotin−avidin system, the multifunctional nanoprobe could conveniently be bound to the glycan sites on the cell surface. The DNA chain presenting between the AuNPs and biotin assembled on the nanoprobe could obviate the steric effect, and HRP acted to trigger the CL emission of the luminal-H_2O_2 system. Therefore the expression of both sialyl and galactosyl groups could be selectively monitored by CL imaging with high sensitivity due to the high amount of HRP. Using human liver cancer HCCC-9810 cells as a model, this CL imaging strategy could detect HCCC cells ranging from 6×10^2 to 1×10^7 cells mL^{-1} with a detection limit down to 12 cells. More importantly, this method could be used for distinguishing cancer cells from normal cells and monitoring of dynamic carbohydrate expression on living cells, providing promising application in clinical diagnosis and treatment of cancer.

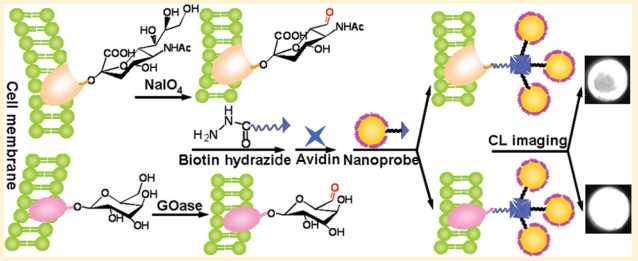

Cell-surface glycans, a large group of biomolecules with diverse structures, play significant roles in many cellular processes, including cell−cell communication, immune recognition/response, cell adhesion, and pathological processes.[1−4] The variations in cell-surface glycans have been demonstrated to be associated with many diseases, such as inflammation and cancers.[5−7] For example, the overproduction of sialyl groups has been found on colorectal cancer cells as compared to normal control.[8] Therefore, the development of sensitive, practical, and high-throughput monitoring methods for analyzing the changes of cell-surface glycans has become an important goal for understanding their roles in disease development and providing diagnostic tools to guide treatment.[9]

It is quite important to choose specific in situ labeling methods for improving the specificity during the detection of cell-surface glycans. The biorecognition of lectins or antibodies to defined glycan specificities has offered valuable tools to label and profile cell-surface glycan expression.[10,11] Lectins have been widely used to analyze glycan expression on cell surfaces, including lectin-array-based microscopic approaches[12−14] and probe-tagged lectin-based electrochemical strategies.[15−17] However, lectin-based methods generally suffer from the poor specificity and low affinity of lectins.[18] Meanwhile, the utilization of biorecognition technology might be hindered by either high cost or relatively poor stability of proteins themselves.[19] To improve the specificity, metabolic oligosaccharide engineering has been introduced as an alternative way to label cell-surface glycans by culturing cells with sugars that contain a bio-orthogonal functional group and expressing this group on the cell surfaces through metabolic processes.[20,21] However, this technique cannot be easily applied to clinical samples because of the time-consuming sugar precursor incubation step prior to labeling.

Recently, chemical and enzymatic oxidization for highly stable, specific, and selective glycan-labeling by specific covalent bond has widely been concerned.[22−27] These strategies mainly include phenylboronic acid recognition[22,23] and an aldehyde tag.[24−27] Phenylboronic acid, a synthetic molecule, has been demonstrated to form stable binding with the sialyl group.[22,23] The aldehyde tag can be formed by specific oxidization of the hydroxyl sites of sialyl and galactosyl groups on cell surfaces.[24,27] Because aldehydes are otherwise absent from mammalian cell surfaces, this process can introduce a unique functional group onto the cell surface, which can then be chemoselectively tagged by treatment with a hydrazine to yield a hydrazone.[28]

Besides the enhanced stability and specificity, the amplification of signal is also an object to improve the analytical performance. This object is often achieved by assembling biomolecules such as enzymes on gold nanoparticles (AuNPs) to construct biological nanoprobes.[29,30] These nanoprobes have been used in various sensing and imaging platforms.[31−34] The combination of AuNP-based probe with different imaging

Received: October 1, 2011
Accepted: January 3, 2012
Published: January 3, 2012

   dx.doi.org/10.1021/ac203489e | *Anal. Chem.* 2012, 84, 1452−1458

Scheme 1. Schematic Representation of (A) Nanoprobe Assembly and (B) CL Imaging for Analysis of Cell Surface Glycan Expression

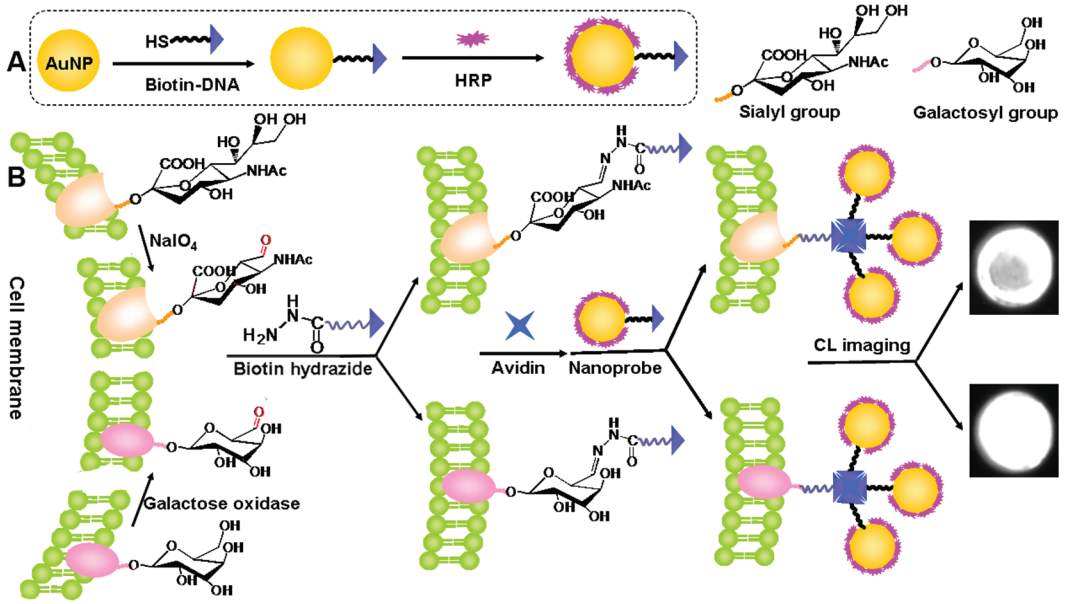

techniques can greatly improve the detection sensitivity, precision, and reproducibility. This work utilizes the high surface-to-volume ratio of AuNPs to assemble a multifunctional nanoprobe for chemiluminescent (CL) imaging. As the Pluronic NP-based near-infrared CL imaging of biologically generated hydrogen peroxide in vivo[35] and other imaging platforms, the introduction of a AuNP-based probe into CL imaging for the cell surface glycan assay will not only contribute to the enhancement of detection sensitivity and obviate the need of cell lysis or complicated instrumentation involved in existing methods but also provide a high-throughput monitoring method for glycan analysis. The integration of enzyme-functionalized AuNPs with a biorecognition element endows the nanoprobe with multiple ability including specific recognition and signal amplification of CL emission.

The recognition element of the designed nanoprobe is the specific binding of biotin to avidin. The biotin group is bound to AuNPs by a DNA chain, and the avidin-labeled glycan sites are formed on the cell surface by an aniline-catalyzed hydrazone ligation of aldehyde with biotin hydrazide. After the recognition of the nanoprobe to the avidin-labeled glycan sites, the horseradish peroxidase (HRP) assembled on the nanoprobe can trigger the CL emission to produce amplified signal for CL imaging. Thus, a sensitive CL imaging method for in situ monitoring of cell-surface glycan expression is developed by combining the specifically chemical and enzymatic oxidization of glycan on cells with the multifunctional nanoprobe. This CL imaging strategy can sensitively detect cells down to 12 HCCC cells with a broad linear range. The proposed chemoselective method can be used for distinguishing cancer cells from normal cells and monitoring dynamic carbohydrate expression on living cells. It would contribute considerably to meeting the challenges in comprehensive understanding of the glycomic codes.

EXPERIMENTAL SECTION

Reagents. Sialidase, sialic acid, biotin hydrazide, avidin, fluorescein isothiocyanate (FITC)-labeled avidin, galactose, galactose oxidase, and bovine serum albumin (BSA) were purchased from Sigma-Aldrich Inc. $AuCl_3HCl{\cdot}4H_2O$ (>48% Au) and sodium citrate were obtained from Shanghai Chemical Reagent Co., Ltd. (China). Biotin-DNA (5′-biotin-GAGTTGTCGGTGTAGGTCG-$(CH_2)_3$-SH-3′) was synthesized by Shanghai Sangon Biotechnology Co., Ltd. (China). Horseradish peroxidase (HRP) and CL substrate solutions (luminol-*p*-iodophenol and H_2O_2) were purchased from Nanjing Sunshine Bio Co., Ltd. (China). Sodium periodate ($NaIO_4$) was purchased from Alfa Aesar China Ltd. 3-(4,5-Dimethylthiazol-2-yl)-2,5-diphenyltetrazolium bromide (MTT) was obtained from Nanjing KeyGen Biotech. Co., Ltd. (China). Aniline was purchased from Sinopharm Chemical Reagent Co., Ltd. (China). All other reagents were of analytical grade. Phosphate buffered saline (PBS, 0.01 M, pH 7.4) contained 136.7 mM NaCl, 2.7 mM KCl, 8.7 mM Na_2HPO_4, and 1.4 mM KH_2PO_4. All aqueous solutions were prepared using ultrapure water (≥18 MΩ, Milli-Q, Millipore).

Apparatus. The UV−vis absorption spectra were recorded with an UV-3600 UV−vis-near-infrared (NIR) spectrophotometer (Shimadzu, Japan). CL spectral responses were recorded on a RF-5301 PC spectrofluorometer (Shimadzu, Japan). The transmission electron microscopic (TEM) image was observed on a JEM-2100 transmission electron microscope (JEOL Ltd., Japan). Flow cytometric analysis was performed on a FACS Calibar flow cytometer (Becton Dickinson). CL images were obtained using an EC3 imaging system with a thermoelectrically cooled CCD camera (UVP).

Cell Culture and Treatment. HCCC-9810, BEL-7405, and QSG-7710 cells were obtained from the Cell Bank of Chinese Academy of Sciences (Shanghai, China). All cells were cultured in a flask in RPMI 1640 medium (GIBCO) supplemented with 10% fetal calf serum (FCS, Sigma), penicillin (100 μg mL^{-1}), and streptomycin (100 μg mL^{-1}) at 37 °C in a humidified atmosphere containing 5% CO_2. The cells in the exponential growth were collected and separated from the medium by centrifugation at 1000 rpm for 5 min and then washed thrice with sterile 10 mM pH 7.4 PBS. The sediment was resuspended in 10 mM pH 7.4 PBS to obtain a

dx.doi.org/10.1021/ac203489e | *Anal. Chem.* 2012, 84, 1452−1458

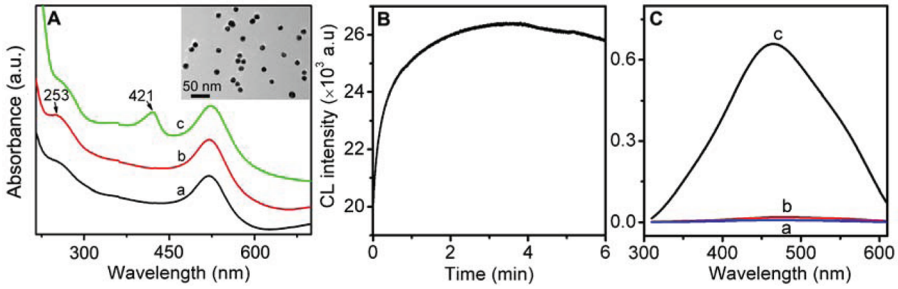

Figure 1. (A) UV−vis spectra of (a) AuNPs, (b) biotin-DNA-AuNPs, and (c) biotin-DNA-AuNPs-HRP; (B) kinetic curve of CL reaction in the presence of the nanoprobe, and (C) CL spectra recorded with an emission slit of 10 nm from 310 to 610 nm upon addition of 300 μL of CL substrates into 50 μL of (a) AuNPs, (b) biotin-DNA-AuNPs, and (c) biotin-DNA-AuNPs-HRP. Inset in part A, TEM image of biotin-DNA-AuNPs-HRP.

homogeneous cell suspension. The cell number was determined using a Petroff-Hausser cell counter. Sialidase-treated HCCC-9810 cells were obtained by incubating the cells in a culture medium containing 10 μg mL^{-1} sialidase for 18 h.

Preparation of Nanoprobe. The preparation of the nanoprobe was shown in Scheme 1A. AuNPs (13 nm) were prepared by the reduction of $HAuCl_4$ with trisodium citrate according to a previous procedure.[36] An amount of 0.3 mL (1 μM) of biotin-DNA was first added into 5 mL (20 nM) of AuNPs solution. After incubation for 16 h and then salt-stabilization with 0.1 M NaCl, the pH of the colloidal gold solution was adjusted to 9.0 by adding 1 mM of NaOH, and then 0.3 mL of 1 mg mL^{-1} of HRP was added to the upper solution. After incubation for 30 min at 25 °C under gentle stirring, the mixture was washed by centrifugation (10 000 rpm, 30 min, 4 °C) and resuspended with 10 mM pH 7.4 PBS. Subsequently, 1 mL of 1% BSA solution was added in the solution with stirring for 30 min to passivate the left active sites on AuNPs. The resulting solution was centrifuged at 10 000 rpm at 4 °C for 30 min, and the supernatant was removed. The final nanoprobe was resuspended in 10 mM PBS at pH 7.4 containing 0.1 M NaCl and stored in a refrigerator at 4 °C for further use.

Cell Surface Glycan Analysis. An amount of 40 μL of cells at different concentrations were seeded in microplate wells and incubated for 4 h under the same conditions as those for the cell culture. After the culture solution was removed, the microplate wells were blocked with 1% BSA for 30 min and washed thrice with pH 7.4 PBS. A solution of 50 μL of 1 mM $NaIO_4$ was added to each microplate well for 30 min at 4 °C to perform the oxidation of sialyl groups on cells, and 50 μL of 3 U mL^{-1} galactose oxidase was added to each microplate well for 1 h at 37 °C for the oxidation of galactosyl groups on cells. After thrice washing with PBS, 50 μL of the mixture containing 10 mM aniline, 100 μM biotin hydrazide, and 5% FCS was added to each microplate well for 1.5 h at 4 °C. After the microplates were carefully washed thrice with PBS, 50 μL of 0.1 mg mL^{-1} avidin was then added and incubated for 30 min at room temperature. After thrice washing with PBS, the cells in the microplate wells were incubated with 50 μL of 20 nM nanoprobe for 30 min at room temperature. After the microplate wells were carefully washed thrice with PBS, 50 μL of CL substrate solution was added to the microplate wells, and the CL signal could be obtained by the CCD camera after 3 min of exposure.

Colorimetric Detection of Cell Surface Sialic Acid. Cell suspensions (40 μL) were first seeded in microplate wells and incubated for 4 h. After the culture solution was removed, the microplate wells were washed thrice with pH 7.4 PBS, and 0.2 mL of 10 μg mL^{-1} sialidase solution was added to each microplate well for 20 h at 37 °C to cut off the sialyl groups on cells. After thrice washing with 0.1 mL of PBS, all solutions were collected to obtain the sample solution (~0.5 mL) containing the cleaved sialic acid. According to the method described by Juoudian et al.,[37] the solution was mixed with 0.1 mL of 40 mM periodic acid solution and kept in an ice bath for 20 min. Afterward, 1.25 mL of resorcinol was added into the mixture and kept in an ice bath for 5 min. After heating to 100 °C for 15 min and then cooled, it was mixed with 1.25 mL of *tert*-butyl alcohol to give a single phase solution, which was then placed in a 37 °C water bath for 3 min to stabilize the color. The amount of sialic acid was detected using UV−vis spectroscopy at 630 nm.

Flow Cytometric Analysis of Glycan Expression on HCCC Cells. HCCC cells in the exponential growth phase were collected and separated from the medium by centrifugation at 1000 rpm at room temperature for 6 min. After subjected to sequential labeling of cell-surface sialyl groups by biotin hydrazide as mentioned above, the cells were washed with sterile cold pH 7.4 PBS and resuspended in the PBS. The cell concentration was determined. A volume of 50 μL of 1×10^7 cells mL^{-1} cell suspension was then added to the mixture of 445 μL of PBS and 5 μL of 2 mg mL^{-1} FITC-labeled avidin. After incubation for 30 min, the cells were collected by centrifugation at 1000 rpm for 6 min, washed twice with 200 μL of cold PBS, resuspended in 500 μL of PBS, and assayed by flow cytometry. Unlabeled HCCC cells were used as the control for estimation of autofluorescence, and relative cell-associated fluorescent intensity was obtained by subtraction of autofluorescence.

Cell Viability Assay. The viability of HCCC cells during the sequential labeling processes of cell-surface sialyl and galactosyl groups and after coupling the nanoprobe for different times was evaluated by MTT assay. Briefly, after the HCCC cells ($\sim 1.0 \times 10^4$) were cultivated in 100 μL of medium, each well for 4 h, the medium was discarded. The cells were then subjected to the sequential labeling processes of cell-surface sialyl and galactosyl groups, respectively. Meanwhile, the HCCC cells without labeling were only incubated with an equal culture medium as the control. MTT (20 μL, 5 mg mL^{-1}) was then added to each well. After incubation for 4 h at 37 °C, the medium was removed and 100 μL of dimethyl sulfoxide was added to each well and the cell plate was vibrated for 15 min at room temperature to dissolve the crystals formed by the living cells. Finally, the absorbance of each microplate well was

dx.doi.org/10.1021/ac203489e | *Anal. Chem.* 2012, 84, 1452−1458

measured using Hitachi/Roche System Cobas 6000 (Tokyo, Japan) at 490 nm. The relative cell viability (%) was calculated by $(A_{test}/A_{control}) \times 100$.

RESULTS AND DISCUSSION

Design of Sensitive CL Imaging Strategy. The multifunctional nanoprobe was fabricated by assembling biotin-DNA and HRP on AuNPs (Scheme 1A). The biotin-DNA could recognize avidin-labeled glycan sites on the cell surface and obviate the steric effect due to the existence of a long DNA strand. As shown in Scheme 1B, the hydroxyl sites of the sialyl and galactosyl groups on cell surfaces could be selectively oxidized to form aldehydes by periodate and galactose oxidase, respectively, and the aldehydes could bind to the biotin tag by aniline-catalyzed hydrazone ligation. Thus the nanoprobe could effectively recognize the labeled glycan sites on cells by avidin as a bridge to introduce a high amount of HRP to each glycan site. Through CL imaging, both the glycan expression on the cell surfaces and the amount of cells in the microplate well could be sensitively monitored, providing a specific and sensitive strategy for monitoring the cell concentration and the glycan expression extent on living cells.

Characterization of Nanoprobe. UV−vis spectra were used to demonstrate the successful binding of the biotin-DNA strand and HRP to AuNPs (Figure 1A). The size of AuNPs could be estimated to be 13 nm from the absorption peak at 519 nm (curve a). After the biotin-DNA strand was attached on the surface of the AuNPs, an obvious absorption peak occurred at about 253 nm (curve b), which contributed to the DNA strand, indicating the successful binding of biotin-DNA to the surface of AuNPs. The UV−vis spectrum of HRP and biotin-DNA multifunctionalized AuNPs showed a strong and obvious absorption at about 421 nm and the absorption at 253 nm (curve c). The former could be attributed to the characteristic absorption of HRP, indicating the coexistence of biotin-DNA and HRP on the surface of AuNPs. The TEM photo of the nanoprobe showed a uniform spherical shape and monodispersity (inset in Figure 1A), which indicated that no aggregation of the nanoparticles occurred after the binding of biotin-DNA and HRP onto AuNPs.

Kinetic and Mechanism of the CL Reaction. The kinetic behavior of the CL reaction catalyzed by the nanoprobe was studied with a static method (Figure 1B). The CL reaction occurred immediately upon addition of the CL substrates. The intensity of CL emission increased quickly and reached its maximum value within 3 min. The CL kinetic for the reaction catalyzed by the nanoprobe was similar with that of 4 min for the reaction catalyzed by HRP.[38] In order to acquire the high detection sensitivity, 3 min was set as the exposure time of the CCD camera. A further inspection of CL spectra was performed as shown in Figure 1C. In the absence of HRP, the AuNPs and biotin-DNA-AuNPs could not catalyze the CL substrates to produce a CL signal, thus the CL intensity gave a very low response in the wavelength range from 310 to 610 nm (curves a and b). After the binding of HRP to biotin-DNA-AuNPs, the nanoprobe led to a maximum emission peak at about 460 nm (curve c), which was at the same wavelength as that of HRP-catalyzed luminal-H_2O_2 CL emission.

Condition Optimization for Construction of Nanoprobe. The effect of concentrations of biotin-DNA and HRP for the construction of the nanoprobe was investigated in the presence of 2×10^6 cells mL^{-1} HCCC cells. As shown in Figure 2A, the CL signal increased greatly as the concentration of

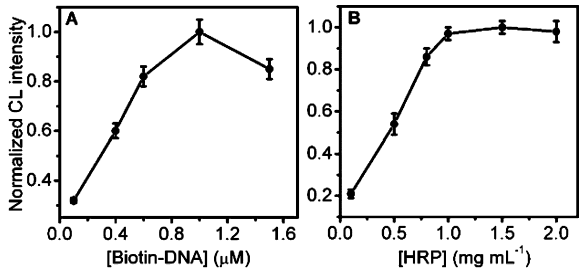

Figure 2. Dependence of the normalized CL intensity for HCCC cells of 2×10^6 cells mL^{-1} on concentrations of (A) biotin-DNA and (B) HRP for preparation of nanoprobes. When one parameter changes, the others are under their optimal conditions.

biotin-DNA changed from 0.1 to 1 μM, followed by a remarkable decrease in the concentration range of 1.0 to 1.5 μM, due to the fact that the excessive biotin-DNA on the nanoprobe decreased the amount of HRP for signal amplification. Therefore, the optimal concentration of biotin-DNA was selected at 1 μM. As shown in Figure 2B, with the increasing HRP concentration from 0.1 to 0.8 μg mL^{-1} for the construction of the nanoprobe, the CL intensity obtained from the biosensor increased greatly. The further increase of HRP concentration did not obviously change the response, indicating that most of the surface sites on AuNPs were already bound sufficiently. Thus, 1 μg mL^{-1} HRP was chosen as the optimal concentration of HRP for the preparation of the nanoprobe.

Signal Amplification and Specificity. Compared with the situation without using the nanoprobe for CL imaging, the nanoprobe produced an about 5 times stronger CL signal at 2×10^6 cells mL^{-1} HCCC cells than that using HRP-avidin for CL imaging (Figure 3A, groups a and b), indicating the CL

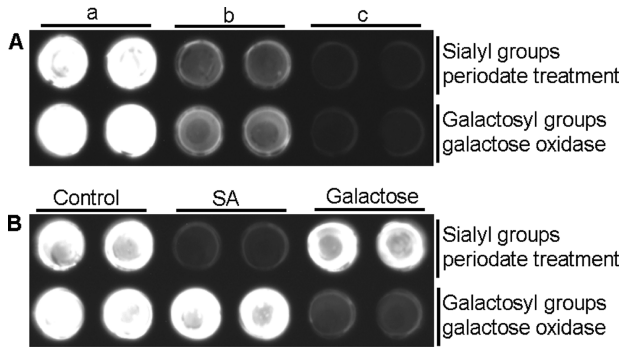

Figure 3. (A) CL images in the presence of nanoprobe (a) and HRP-avidin (b) for 2×10^6 cells mL^{-1} HCCC cells and (c) microplate wells treated with 20 nM nanoprobe in the absence of cells as control, (B) CL images for 2×10^6 cells mL^{-1} HCCC cells in the absence (a) and presence of 5 mM SA (b) or 5 mM galactose (c) to inhibit the oxidation of cell surface glycans by $NaIO_4$ or galactose oxidase solution.

signal amplification ability of the nanoprobe. In the absence of the cells, the microplate wells treated with 20 nM nanoprobe showed neglectable CL response (Figure 3A, group c), indicative of very little nonspecific adsorption of the nanoprobe on the wall of microplate wells. The nanoprobe did not visibly increase the background response, leading to highly sensitive detection.

To validate the specificity of the recognition method by chemical and enzymatic oxidation to label the glycan sites on

dx.doi.org/10.1021/ac203489e | Anal. Chem. 2012, 84, 1452−1458

the cells, the solution of $NaIO_4$ or galactose oxidase was first mixed with 5 mM sialic acid monosaccharide or 5 mM galactose before cell incubation. As shown in Figure 3B, sialic acid and galactose showed an obvious inhibition effect on the labeling of sialyl groups and galactosyl groups on cell surfaces, respectively. This result suggested that the chemical labeling of glycans on living cells was highly selective.

Cell Viability. The viability of HCCC cells during the sequential labeling processes of cell surface sialyl and galactosyl groups was critical to accurately monitor the glycan expression level on living cells. Thus an MTT assay was carried out to evaluate the cell viability during the sequential labeling processes. As shown in Figure 4A, after HCCC cells were

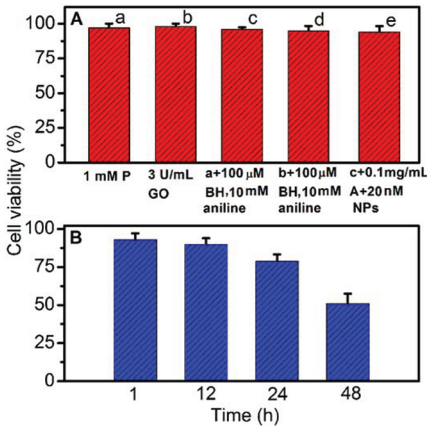

Figure 4. Viability of HCCC cells after (A) treatment in different experimental steps and (B) coupling the nanoprobe for different times. P, periodate; GO, galactose oxidase; BH, biotin hydrazide; A, avidin.

incubated in 1 mM $NaIO_4$ for 30 min or 3 U mL^{-1} galactose oxidase for 1 h, respectively, the cells exhibited very high viability (columns a and b). The subsequent steps for covalent bond formation to bind biotin, recognition of avidin, and even to nanoprobe did not significantly affect the cell viability (column c and e). The HCCC cells could still keep their 94(±4)% viability after the nanoprobe was bound to the cell surfaces by interaction between avidin and biotin (column e). After coupling the nanoprobe for 1 or 12 h, the viability of the cells did not show a statistical change and they could keep 93(±4)% and 90(±3)% viability (Figure 4B). Thus the cells could keep their viability after labeling and quantification for 12 h. These results demonstrated that the designed method and the labeling processes of cell surface glycans did not affect the viability of living cells, although the viability decreased to 51% after coupling the nanoprobe for 48 h.

Cell Detection. Under the optimal conditions, the CL intensity was proportional to the logarithmic value of the cell concentration ranging from 6.0×10^2 to 1.0×10^7 cells mL^{-1} with a correlation coefficient R of 0.998 (Figure 5). The limit of detection for cell concentration was calculated to be 300 cells mL^{-1} at 3σ, which was comparable with that of 750 cells mL^{-1} at a quartz crystal microbalance biosensor for detection of *Escherichia coli*[39] and much lower than that of 6000 cells mL^{-1} at an immunosensor chip for detection of *E. coli* O157:H7,[40] and 1.0×10^4 cells mL^{-1} at an immunosensor for detection of *Salmonella* species based on a quartz crystal microbalance.[41] Taking into account the fact that the volume of HCCC cell suspension for the incubation step was only 40 μL, the

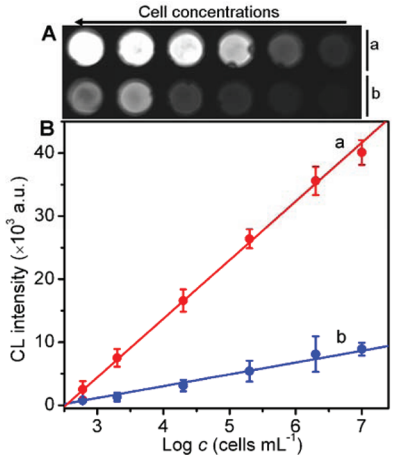

Figure 5. (A) CL images (from right to left, 6.0×10^2, 2.0×10^3, 2.0×10^4, 2.0×10^5, 2.0×10^6, and 1.0×10^7 cells mL^{-1} HCCC cells) and (B) plots of CL intensity vs logarithm of cell concentration for sialyl groups on HCCC cells in the presence of the nanoprobe (a) and HRP-avidin (b).

designed strategy could detect cell numbers down to 12 HCCC cells.

In order to demonstrate the enhanced sensitivity of this nanoprobe-based strategy, the commercially available HRP-avidin was used to replace the nanoprobe for performing the same procedure. Under the same optimal conditions, although the CL intensity increased with the increasing cell concentration (Figure 5B, curve b), the slope of the plot of CL intensity vs logarithmic value of the cell concentration was about 5 times lower than that using the nanoprobe, verifying the advantages of the designed nanoprobe. The enhanced sensitivity could be attributed to the high amount of HRP on the nanoprobe.

The sensitivity of this designed method could be compared with that of the chemical-based colorimetric assay[37] by cleaving the sialic acid from the cell surface. The periodate-resorcinol colorimetric method[37] showed a linear calibration with the logarithmic value of the HCCC cell concentration from 6×10^5 to 1×10^7 cells mL^{-1} with a detection limit of 8×10^3 cells (Figure 6A), indicating much higher sensitivity of the designed

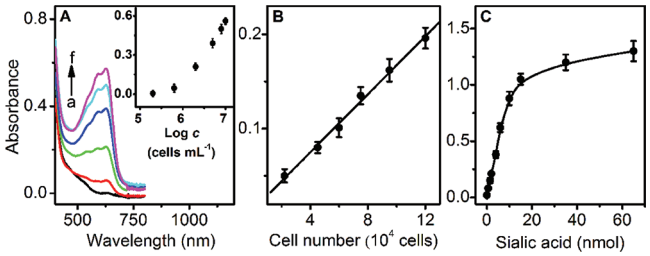

Figure 6. (A) UV–vis spectra of colored products obtained from cleaved sialyl groups with cell concentrations of 2.0×10^5, 6.0×10^5, 2.0×10^6, 7.0×10^6, and 1.0×10^7 cells mL^{-1} (from curves a to f) and plots of UV–vis intensity vs amount of (B) HCCC cells and (C) free sialic acid at the same volume. Inset in part A, plot of UV–vis intensity vs logarithm value of HCCC cell concentration.

method for detection of cells. The absolute sensitivity of the designed method could be obtained by comparing the assay results of two methods. The absorbance linearly increased with the increasing number of HCCC cells from 2.2×10^4 to $1.2 \times$

dx.doi.org/10.1021/ac203489e | *Anal. Chem.* 2012, 84, 1452–1458

10^5 cells (R = 0.998) (Figure 6B), while the linear calibration range for free sialic acid in the solution with the same volume was from 0.1 to 6 nmol (R = 0.997) (Figure 6C). The average number of sialyl groups on single HCCC cell could be estimated to be 9.2×10^9 molecules. Considering the detection limit of 12 HCCC cells, the absolute sensitivity of the designed CL imaging method was calculated to be 0.18 pmol.

Because of the high expression of sialyl and galactosyl groups on the cancer cell surface, this method could be used for distinguish cancer cells from normal cells. As shown in Figure 7,

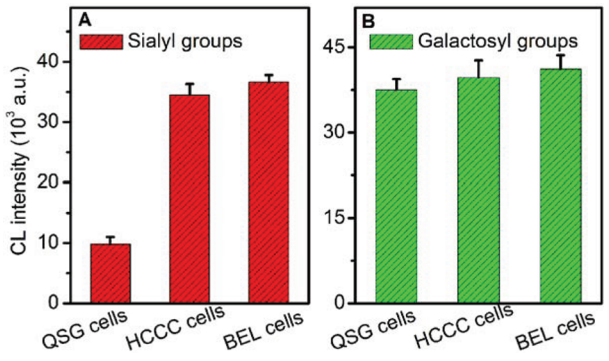

Figure 7. CL intensities corresponded to (A) sialyl and (B) galactosyl expression on normal cells (QSG cells) and cancer cells (HCCC cells and BEL cells) based on the designed strategy with the cell concentration of 2.0×10^6 cells mL^{-1}.

both two kinds of liver cancer cells showed a much higher expression of sialyl group than normal liver cells (Figure 7A), while the expressions of the galactosyl group on three kinds of cells did not show a statistical difference (Figure 7B), which was in good agreement with the previous report.[42] The similar CL responses to the cell surface sialic acid and galactose did not indicate that they are at similar levels due to the different oxidation and labeling efficiency.

At the cell concentrations of 2.0×10^4 and 2.0×10^6 cells mL^{-1}, the CL intensity showed the relative standard deviations of 8.6% and 5.7% examined for five determinations, respectively, showing good reproducibility. Thus, the designed method showed good performance for the detection of living cancer cells with a broad detection range, low detection limit, good reproducibility, and simple detection procedure.

Dynamic Monitoring of Cell Surface Carbohydrate Expression. The high sensitivity and facility of the proposed strategy allowed it to be further used in monitoring of the dynamic alteration of carbohydrate expression on living cells in response to sialidase. Sialidase is usually utilized as a cleaving agent for all forms of sialyl groups present in cell surface glycans.[43] During treatment with sialidase over 18 h, the sialidase-treated cells revealed a progressively decreased change of response compared to untreated cells as a control (Figure 8). This result indicated the decrease of terminal SA on sialidase-treated HCCC cells. After treatment for 18 h, the sialyl groups on sialidase-treated HCCC cells decreased by 91%. This value was compatible with that of 95% obtained from flow cytometric analysis using FITC-labeled avidin for recognition (inset in Figure 8B), suggesting acceptable reliability of the proposed method for dynamic monitoring of cell-surface carbohydrates.

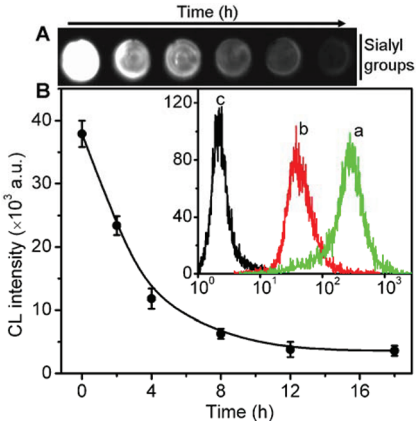

Figure 8. (A) CL images for 2.0×10^6 cells mL^{-1} HCCC cells treated with sialidase for different times and (B) plot of CL intensity vs treatment time. Inset in part B, flow cytometric analysis of sialyl expression on HCCC cells (a) before and (b) after sialidase treatment for 18 h with FITC-labeled avidin and (c) autofluorescence of unlabeled cells.

CONCLUSIONS

This work develops a novel CL imaging method for high-throughput detection of cancer cells and in situ monitoring of cell-surface sialyl expression. By combining the specifically chemical and enzymatic oxidization of glycans on cells for binding of the biotin group with the multifunctional nanoprobe, the proposed method is chemoselective and highly sensitive. The multifunctional nanoprobe fabricated by assembling biotin-DNA and HRP on AuNPs can effectively bind to avidin labeled glycan sites on cells to trigger the CL emission. This CL imaging strategy can be used for sensitive analysis of living cell number with a broad linear range, high specificity, and acceptable reproducibility. It has been used for sensitively distinguishing cancer cells from normal cells and monitoring dynamic carbohydrate expression on living cells. Owing to the high sensitivity and low limit of detection, the proposed strategy could be expanded to the array with more wells to achieve high throughput screening of cell surface sialyl change. This work affords a promising protocol for meeting the challenges in elucidation of the complex mechanisms underlying carbohydrate-related biological processes.

AUTHOR INFORMATION

Corresponding Author

*Phone/fax: +86-25-83593593. E-mail: hxju@nju.edu.cn.

ACKNOWLEDGMENTS

We gratefully acknowledge the National Basic Research Program of China (Grant 2010CB732400), National Natural Science Foundation of China (Grants 21005037, 21135002, and 21121091), PhD Fund for Young Teachers (Grant 20100091120034), the Fundamental Research Funds for the Central Universities (Grant 1117020501), and the Natural Science Foundation of Jiangsu (Grant BK2010193).

REFERENCES

(1) Rudd, P. M.; Elliott, T.; Cresswell, P.; Wilson, I. A.; Dwek, R. A. *Science* **2001**, *291*, 2370−2376.
(2) Ohtsubo, K.; Marth, J. D. *Cell* **2006**, *126*, 855−867.
(3) Marth, J. D.; Grewal, P. K. *Nat. Rev. Immunol.* **2008**, *8*, 874−887.

(4) Kinjo, Y.; Wu, D.; Kim, G.; Xing, G.-W.; Poles, M. A.; Ho, D. D.; Tsuji, M.; Kawahara, K.; Wong, C.-H.; Kronenberg, M. *Nature* **2005**, *434*, 520−525.
(5) Crocker, P. R.; Feizi, T. *Curr. Opin. Struct. Biol.* **1996**, *6*, 679−691.
(6) Bertozzi, C. R.; Kiessling, L. L. *Science* **2001**, *291*, 2357−2364.
(7) Dube, D. H.; Bertozzi, C. R. *Nat. Rev. Drug Discovery* **2005**, *4*, 477−488.
(8) Qiu, Y.; Patwa, T. H.; Xu, L.; Shedden, K.; Misek, D. E.; Tuck, M.; Jin, G.; Ruffin, M. T.; Turgeon, D. K.; Synal, S.; Bresalier, R.; Marcon, N.; Brenner, D. E.; Lubman, D. M. *J. Proteome Res.* **2008**, *7*, 1693−1703.
(9) Krishnamoorthy, L.; Mahal, L. K. *ACS Chem. Biol.* **2009**, *4*, 715−732.
(10) Lis, H.; Sharon, N. *Chem. Rev.* **1998**, *98*, 637−674.
(11) Agard, N. J.; Bertozzi, C. R. *Acc. Chem. Res.* **2009**, *42*, 788−797.
(12) Hsu, K.; Pilobello, K. T.; Mahal, L. K. *Nat. Chem. Biol.* **2006**, *2*, 153−157.
(13) Pilobello, K. T.; Slawek, D. E.; Mahal, L. K. *Proc. Natl. Acad. Sci. U.S.A.* **2007**, *104*, 11534−11539.
(14) Zheng, T.; Peelen, D.; Smith, L. M. *J. Am. Chem. Soc.* **2005**, *127*, 9982−9983.
(15) Cheng, W.; Ding, L.; Ding, S. J.; Yin, Y. B.; Ju, H. X. *Angew. Chem., Int. Ed.* **2009**, *48*, 6465−6468.
(16) Cheng, W.; Ding, L.; Lei, J. P.; Ding, S. J.; Ju, H. X. *Anal. Chem.* **2008**, *80*, 3867−3872.
(17) Ding, L.; Ji, Q. J.; Qian, R. C.; Cheng, W.; Ju, H. X. *Anal. Chem.* **2010**, *82*, 1292−1298.
(18) Kohler, J. J. *ChemBioChem* **2009**, *10*, 2147−2150.
(19) Xu, H.; Mao, X.; Zeng, Q.; Wang, S.; Kawde, A.-N.; Liu, G. *Anal. Chem.* **2009**, *81*, 669−675.
(20) Dube, D. H.; Bertozzi, C. R. *Curr. Opin. Chem. Biol.* **2003**, *7*, 616−625.
(21) Prescher, J. A.; Bertozzi, C. R. *Cell* **2006**, *126*, 851−854.
(22) Matsumoto, A.; Cabral, H.; Sato, N.; Kataoka, K.; Miyahara, Y. *Angew. Chem., Int. Ed.* **2010**, *49*, 5494−5497.
(23) Han, E.; Ding, L.; Ju, H. X. *Anal. Chem.* **2011**, *83*, 7006−7012.
(24) Zeng, Y.; Ramya, T. N. C.; Dirken, A.; Dawson, P. E.; Paulson, J. C. *Nat. Methods* **2009**, *6*, 207−109.
(25) Nilsson, J.; Ruetschi, U.; Halim, A.; Hesse, C.; Carlsohn, E.; Brinkmalm, G.; Larson, G. *Nat. Methods* **2009**, *6*, 809−813.
(26) Wollscheid, B.; Bausch-Fluch, D.; Henderson, C.; Brien, R.; Bibel, M.; Schiess, R.; Aebersold, R.; Watts, J. D. *Nat. Biotechnol.* **2009**, *27*, 378−386.
(27) Rannes, J. B.; Ioannou, A.; Willies, S. C.; Grogan, G.; Behrens, C.; Flitsch, S. L.; Turner, N. J. *J. Am. Chem. Soc.* **2011**, *133*, 8436−8439.
(28) Prescher, J. A.; Bertozzi, C. R. *Nat. Chem. Biol.* **2005**, *1*, 13−21.
(29) Katz, E.; Willner, I. *Angew. Chem., Int. Ed.* **2004**, *43*, 6042−6108.
(30) Rosi, N. L.; Mirkin, C. A. *Chem. Rev.* **2005**, *105*, 1547−1562.
(31) Nam, J.-M.; Thaxton, C. S.; Mirkin, C. A. *Science* **2003**, *301*, 1884−1886.
(32) Qiu, F.; Jiang, D.; Ding, Y.; Zhu, J.; Huang, L. L. *Angew. Chem., Int. Ed.* **2008**, *47*, 5009−5012.
(33) Jiang, Y.; Zhao, H.; Zhu, N. N.; Lin, Y. Q.; Yu, P.; Mao, L. Q. *Angew. Chem., Int. Ed.* **2008**, *47*, 8601−8604.
(34) Li, J.; Song, S. P.; Liu, X. F.; Wang, L. H.; Pan, D.; Huang, Q.; Zhao, Y.; Fan, C. H. *Adv. Mater.* **2008**, *20*, 497−500.
(35) Lim, C. K.; Lee, Y. D.; Na, J.; Oh, J. M.; Her, S.; Kim, K.; Choi, K.; Kim, S.; Kwon, I. C. *Adv. Funct. Mater.* **2010**, *20*, 2644−2648.
(36) Ambrosi, A.; Castañeda, M. T.; Killard, A. J.; Smyth, M. R.; Alegret, S.; Merkoçi, A. *Anal. Chem.* **2007**, *79*, 5232−5240.
(37) Jourdian, G. W.; Dean, L.; Roseman, S. *J. Biol. Chem.* **1971**, *246*, 430−435.
(38) Fu, Z. F.; Liu, H.; Ju, H. X. *Anal. Chem.* **2006**, *78*, 6999−7005.
(39) Shen, Z. H.; Huang, M. C.; Xiao, C. D.; Zhang, Y.; Zeng, X. Q.; Wang, P. G. *Anal. Chem.* **2007**, *79*, 2312−2319.
(40) Ruan, C. M.; Yang, L. J.; Li, Y. B. *Anal. Chem.* **2002**, *74*, 4814−4820.
(41) Wong, Y. Y.; Ng, S. P.; Ng, M. H.; Si, S. H.; Yao, S. Z.; Fung, Y. S. *Biosens. Bioelectron.* **2002**, *17*, 676−684.
(42) Zhang, X. N.; Teng, Y. Q.; Fu, Y.; Xu, L. L.; Zhang, S. P.; He, B.; Wang, C. G.; Zhang, W. *Anal. Chem.* **2010**, *82*, 9455−9460.
(43) Fukuda, M.; Bao, X. F. *Nat. Chem. Biol.* **2008**, *4*, 721−722.